



# SARIMA-Based Prediction of Chalous River Flow Rates

Zahra Sheikholeslami <sup>1\*</sup>, Majid Ehteshami <sup>2</sup>, Zeinab Ghasemi <sup>3</sup>

<sup>1</sup> PhD in Environmental Engineering, Department of Civil Engineering, K.N. Toosi University of Technology, Tehran, Iran.

<sup>2</sup> Associate Professor of Department of Civil Engineering, K.N. Toosi University of Technology, Tehran, Iran.

<sup>3</sup> PhD Candidate of Environmental Engineering, Department of Civil and Environmental Engineering University of Auckland, Auckland, New Zealand.

## Article Info

Received 1 August 2024

Accepted 25 August 2024

Available online 1 September 2024

## Keywords:

SARIMA;

Prediction;

River Flow Rate;

ACF;

PACF;

Time Series.

## Abstract:

The monthly flow rates of the Chalus River in Mazandaran Province, Iran are predicted using the Seasonal Autoregressive Integrated Moving Average (SARIMA) model in this research. The SARIMA model was created and verified with MiniTab software by analyzing historical data spanning from 2006 to 2023. The modeling process involved checking data stationarity with the Augmented Dickey-Fuller (ADF) test, normalizing data using the Johnson Transformation, and determining the best SARIMA parameters by analyzing Autocorrelation Function (ACF) and Partial Autocorrelation Function (PACF) plots. The SARIMA model with parameters (2,0,0)(0,1,1)<sub>12</sub> was determined to be the most precise in predicting future outcomes, exhibiting a strong  $R^2$  value and reliable forecasting capabilities. Despite effectively modeling the seasonal changes of the Chalus River, the model proved to be inadequate in predicting extreme flow rates. The findings indicate that utilizing the SARIMA model proves to be a dependable instrument for overseeing water resources in the area, with potential for further investigation into integrating SARIMA with alternative approaches to improve forecasting of exceptional occurrences.

© 2024 University of Mazandaran

\*Corresponding Author: [zsheikholeslami@email.kntu.ac.ir](mailto:zsheikholeslami@email.kntu.ac.ir)

**Supplementary information:** Supplementary information for this article is available at <https://cste.journals.umz.ac.ir/>

**Please cite this paper as:** Sheikholeslami, Z., Ehteshami, M., & Ghasemi, Z. (2024). SARIMA-Based Prediction of Chalous River Flow Rates. Contributions of Science and Technology for Engineering, 1(3), 1-9. doi:10.22080/cste.2024.27633.1001.

## 1. Introduction

Water management decision making process requires accurate forecasts of the short-term water demand. This short-term water demand forecast can be used in the areas of water reservoir design, future studies, and quality distribution problems [1]. Precise predictions of river flow are essential for various water management systems such as irrigation projects, urban development plans, and flood control strategies [2-4]. Chalus River as shown in Figure 1 is a significant river of central-northern of Iran which located in the west of Mazandaran province, and originates from the northern slopes of the Kandavan and Taleghan highlands and flows into the Caspian Sea after traveling about 85 kilometers along the Chalus near Deh Farajabad. This river with its main branch Hanisak, Makaroud, Dalir and Barar and its sub-branches has a catchment area of 1550 square kilometers. The course of this river is mountainous and the river bed is narrow and its flow is rapid and torrential [5].

The Chalous River plays a vital role in the environmental, economic, and social aspects of the region through critical applications such as agricultural irrigation, drinking water

supply, hydropower generation, flood control, tourism and recreation, and environmental conservation. Due to the importance of Chalous River it is essential to utilize scientific methods to forecast the future River flow accurately, by using historical data to assist water management company and authorities in decision-making [1].

Hydrological data are frequently subject to the influence of numerous external factors, resulting in time series that demonstrate both linear and nonlinear behaviors [6]. For analyzing and forecasting the hydrologic time series in recent years, the BoxJenkins time series analysis techniques, such as auto-regressive (AR), moving average (MA), autoregressive moving average (ARMA), autoregressive integrated moving average (ARIMA), and seasonal autoregressive integrated moving average (SARIMA) have been the primary methods employed [7]. The SARIMA model is advantageous due to its ability to consider both seasonal and non-seasonal patterns, giving it an edge over ARIMA. However, it is constrained by the necessity of having a minimum of 50 past data points and achieving precise forecasts in a brief timeframe [8-10].



ISSN 3060-6578

© 2024 by the authors. Licensee CSTE, Babolsar, Mazandaran. This article is an open access article distributed under the terms and conditions of the Creative Commons Attribution (CC-BY) license (<https://creativecommons.org/licenses/by/4.0/deed.en>)

SARIMA models have been previously employed with success in predicting hydrological patterns, as evidenced by Gharde et al. (2016) who utilized a SARIMA model for forecasting Streamflow in the Savitri Basin. Their model performance in diagnostic and calibration stages was satisfactory, with R value  $> 0.9$ , low RMSE, CE nearing 100, and EV low. This suggests the model's suitability for daily streamflow forecasting with strong short-term performance [11]. Katimon et al. (2017) developed stochastic models to predict Johor river water quality and hydrological variables in Malaysia. They found that the models are beneficial for addressing rapid land use changes and can help investigate the relationship between water quality and rainfall-runoff processes [12]. Kassem et al. (2020) predicted the daily streamflow of Khazir River Basin by using SARIMA and ANN models, finding that both the SARIMA and ANN-MLP models demonstrated similar level of performance, with ANN-MLP showing slightly better accuracy [13]. Adams and Bamanga (2020) proposed a SARIMA model to predict monthly rainfall in Abuja, Nigeria from 1996 to 2018. The model was used to forecast rainfall for the next four years, indicating a 3.5% increase in rainfall from 2018 to 2019, 4.9% from 2018 to 2020, 4.7% from 2018 to 2021, and 5.2% from 2018 to 2022 [14]. Liu et al. (2023) investigated the hydrological data of a hydrothe paperr station in Xiaolangdi Reservoir over the past six years. The SARIMA model and CUSUM algorithm were used to analyze the multi-scale hydrological characteristics of the station. Results show that the

seasonality, periodicity, and mutation of water and sand flux in the area reveal a strong correlation between rainfall and seasonal changes [15]. Ning and Musa (2023) used time series models, ARIMA, ARMA, and SARIMA to forecast two stations, Temerloh and Lubok Paku, of Pahang River. SARIMA is chosen as the best model, generating high accuracy with a MAPE of 18.35% for Temerloh and 6.54% for Lubok Paku, and improved forecasting precision due to seasonality [16]. Sheikholeslami et al. (2024) modeled the Karaj Dam reservoir in Tehran's water supply system by using Historical data from April 2006 to March 2022 to predict the reservoir's share in Tehran's water supply for April 2023 to March 2023. The SARIMA model was chosen for Tehran's water consumption and inflow prediction. The model results showed a decrease in reservoir volume, affecting household water supply and agricultural usage [10].

The objective of this research is to utilize SARIMA modeling on historical flow data of the Chalus River. The purpose is to assess the model's effectiveness in predicting future flow rates and to provide valuable insights for water management decisions in the region. The implementation of SARIMA predictions enables local authorities to improve their capacity to forecast and alleviate the consequences of seasonal fluctuations and extreme weather events on river discharge in Mazandaran province, thereby supporting the sustainable management of water resources.

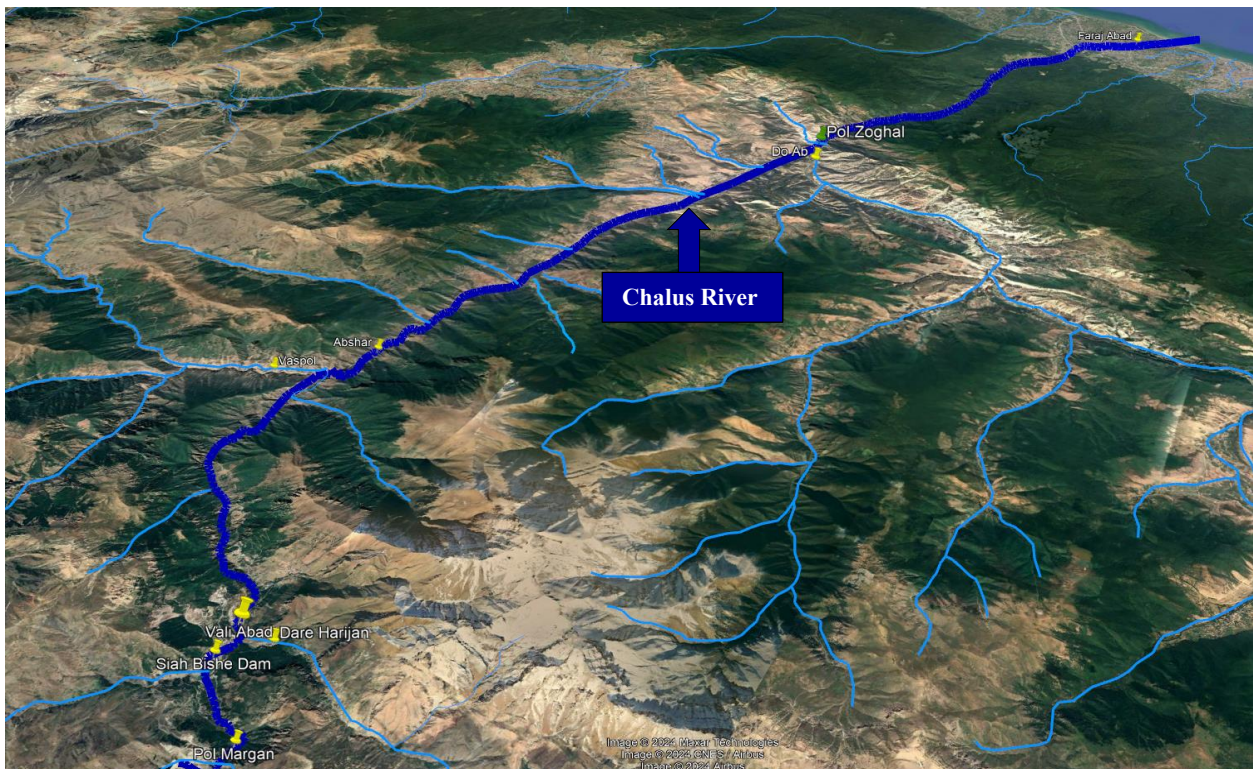


Figure 1. Path of the Chalus River by Google Earth

## 2. Materials and Methods

### 2.1. Study Area

The Chalus River plays a crucial role as a surface water source in the western region of Mazandaran Province, Iran.

The river's flow rate is continuously monitored by seven measurement stations, which are essential for managing water resources effectively in the area. These monitoring stations are essential for comprehending the river's patterns throughout various seasons, which is vital for managing

floods, planning irrigation, and securing a consistent water source for nearby regions [17]. Table 1 provides an

overview of the monitoring stations situated on Chalus River, as shown in Figure 1.

**Table 1. The overview of the monitoring stations**

Number	Monitoring Stations	Geographic Coordinates		The Length Of The Main Branch Of The River (Km)	Area Of Watershed (Km <sup>2</sup> )
		Y	X		
1	Pol Margan	4007103	529653	9.1	59.306
2	Darre Harijan	4009745	528388	14.6	84.839
3	Vali Absd	4009893	527207	19.6	181.099
4	Vaspoul	4018385	520707	24.3	302.191
5	Abshar	4020628	522969	27.6	586.186
6	Do Ab	4038907	530264	42.9	627.434
7	Pol Zoghal	4040624	529799	50.1	1583.362

The main station on Chalus River, Pol Zoghal, has been chosen to analyze the monthly data spanning from 2006 to 2023 in order to forecast the river's flow rate for the entire year of 2024 through SARIMA modeling conducted on Minitab software.

## 2.2. SARIMA Model

The flowchart illustrating the procedure for time series modeling can be found in Figure 2. The primary stages of time series modeling involve identifying the model, estimating parameters, conducting diagnostic checks, and making forecasts.

Box-Jenkins made a notable impact on time series forecasting by introducing a general approach and emphasizing the importance of data stationarity as a primary condition for effective time series modeling. If the data is non-stationary, steps should be taken to achieve stationarity before modeling [18]. Stationary time series exhibit constant mean and variance values, which is investigated by Augmented Dicky Fuller Test (ADF), which assesses stationarity by detecting the presence or absence of a unit root. If a time series is non-stationary and demonstrates a trend, it can be made stationary by identifying and eliminating instability factors directly, as well as utilizing transformation and differentiation functions [19].

Besides being stationary, the series must also exhibit a Normal distribution. The normality of a time series can be examined using statistical methods such as Kolmogorov-Smirnov, Anderson-Darling, and Shapiro-Wilk tests. In this study, the Anderson-Darling method was employed to evaluate the normal distribution of the Chalus River time series data. In this assessment, a P-Value lower than 0.05 leads to the dismissal of the null hypothesis regarding the normality of the data, indicating the non-normality of the time series data, therefore, it is crucial to normalize the time series prior to modeling through the application of transformation functions [10].

Alongside evaluating the normality of the data, it is vital to examine trend and homogeneity of time series in the discussion of data stationarity. The Mann-Kendall trend test, a nonparametric technique based on ranks, is

commonly utilized to identify trends in Hydrological time series due to its resilience to outliers [20], as demonstrated by Jin et al (2018) where Mann-Kendall trend analysis is a widely accepted approach for studying Hydrological variability [21]. The null hypothesis ( $H_0$ ) of the Mann-Kendall test ) states that there is no trend in time series and the p-value higher than the significance level  $\alpha=0.05$ , cannot reject the null hypothesis [22]. The purpose of homogeneity tests is to ascertain whether the variations are linked to a change in the average. The commonly used methods for assessing homogeneity include the Standard normal homogeneity test, Pettitt test, Buishand range test, and Von Neumann ratio test, which in this study the Pettitt test is employed to assess homogeneity for recognizing the change point [23]. The null hypothesis ( $H_0$ ) of Pettitt test asserts the data are homogenous, which rejected by the p-value lower than 0.05 [10].

Following the standardization of the data, the model order and parameters were estimated by analyzing the autocorrelation function (ACF) and partial autocorrelation function (PACF) charts. The ACF and partial PACF plots were employed as valuable instruments to verify stationarity, recognize the SARIMA model structures, and determine the order of p, P, q, and Q. By trying out various orders of repetitive processes, the model with the lowest Akaike Information Criterion (AIC) value was identified as the most appropriate model. Subsequently, the accuracy of the model was assessed through the Anderson Darling test for normality of residuals, Chi-Square test for data independence, and the Run Test for data randomness. Finally to evaluate the accuracy of the results obtained from the models, the relationships in Table 2 have been used.

## 3. Results

The prediction of the Chalous River's flow rates was achieved through the application of the SARIMA model, which took into consideration seasonal features in the time series data within MiniTab software. The analysis and forecasting of time series data on Chalous River flow rates provide essential insights for urban planners and researchers, enabling them to estimate future consumption

values and identify main parameters such as trends, seasonal effects, and jumps through the application of models.

Initially, the stationary and normality of the Chalus River time series data were assessed using Augmented Dickey-Fuller and Anderson-Darling normality tests with the results outlined in Table 3. In the Augmented Dickey-Fuller test, if the p-value is below 0.05, the null hypothesis of non-stationarity in the time series is rejected, hence it is evident from the test findings and the p-value of 0.0001 that the

Chalus River time series demonstrates stationarity. Since the p-value from the Anderson-Darling test on the Chalus River time series is below 0.05, it indicates that the data does not adhere to a normal distribution. Therefore, in accordance with the normality principle, it is essential to normalize the time series when analyzing and forecasting time series data. Table 4 displayed the transformation functions that were considered for normalizing the time series

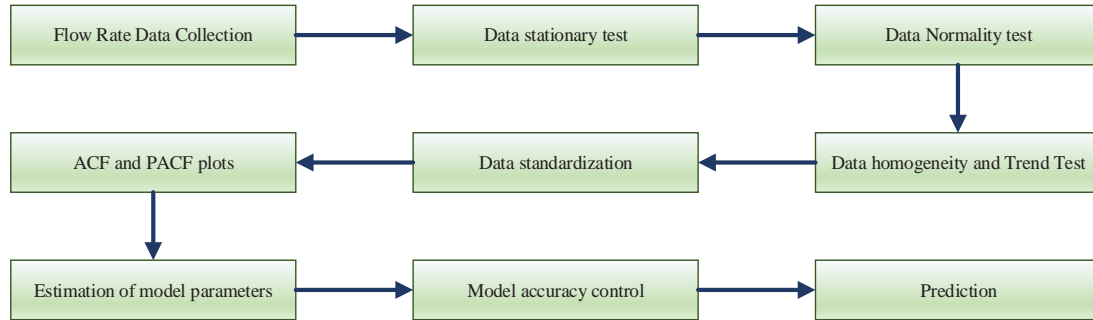


**Figure 2. Flowchart of Time Series Modeling**

**Table 2. The model precision criteria**

Coefficient of determination	Error	Nash Sutcliffe model efficiency coefficient
$R^2 = \frac{(\sum_1^n X_{pi} X_{mi})^2}{\sum_1^n X_{pi}^2 \sum_1^n X_{mi}^2}$	$\%E = \frac{\sum_1^n X_{mi} - X_{pi}}{\sum_1^n X_{mi}}$	$NS = 1 - \frac{\sum_1^n (X_{mi} - X_{pi})^2}{\sum_1^n (X_{pi} - \bar{X}_p)^2}$
$X_p$ =estimated values of the model $X_m$ =observed values,		$\bar{X}_p$ = the average of the observed values $N$ = the number of data.

**Table 3. P-values of statistical tests of Chalous River's flow rate time series**

Pettitt's Test	Mann-Kendall Tests	Augmented Dickey-Fuller Test	Anderson-Darling Normality test
0.2	0.81	0.0001	0.0005

**Table 4. Transformation identification Chalous River's flow rate**

Distribution	P-values
Normal	<0.005
Box-Cox Transformation	<0.005
Lognormal	<0.005
Exponential	<0.003
2-Parameter Exponential	<0.010
Weibull	<0.010
3-Parameter Weibull	<0.005
Smallest Extreme Value	<0.010
Largest Extreme Value	<0.010
Gamma	<0.005
Logistic	<0.005
Loglogistic	<0.005
Johnson Transformation	0.182

Out of the various transformation identification functions, the Johnson Transformation function was selected as the most suitable method for normalizing the data, as the p-value from the Anderson-Darling test exceeded 0.05, in accordance with Equation 1.

$$\text{Johnson transformation function} = -1.06618 + (0.81533 \times \text{LN}(X - 4.0623)) \quad (1)$$

where X is Chalous River's flow rates.

Following the Johnson Transformation, it is evident from the outcomes that the p-value of 0.182 exceeds 0.05, leading to the rejection of the null hypothesis in the Anderson-Darling test, indicating conformity of the transformed data to the normal distribution.

Besides normalizing the data, the homogeneity and trend of the time series data of Chalus River were investigated using Pettit and Mann-Kendall tests. The null hypothesis in Pettitt's test indicated that the p-value of 0.2 supported the homogeneity of Chalus River data. Moreover, in accordance with the Mann-Kendall test result, the p-value of 0.81 exceeding 0.05 supports the null hypothesis, demonstrating the lack of a trend in the time series.

Standardizing the time series of Chalus River is the initial step in preparing the data for modeling, followed by fitting the suitable model to the standardized series. The values for SARIMA (p, d, q)(P, D, Q) were determined through the analysis of ACF and PAC) plots. The value of component d in the Chalus River time series is zero because considering to the Mann-Kendall test result, there is no trend observed.

Conversely, as shown in Figure 3-a, the appearance of a repeating sine wave in the ACF plot indicates that the time series being analyzed exhibits a seasonal pattern with a cycle of 12. The seasonal component was eradicated

through the use of first-order seasonal differentiation, and subsequently, the repeating sine wave in the ACF diagram was removed as shown in Figure 4-a, resulting in a value of D being one.

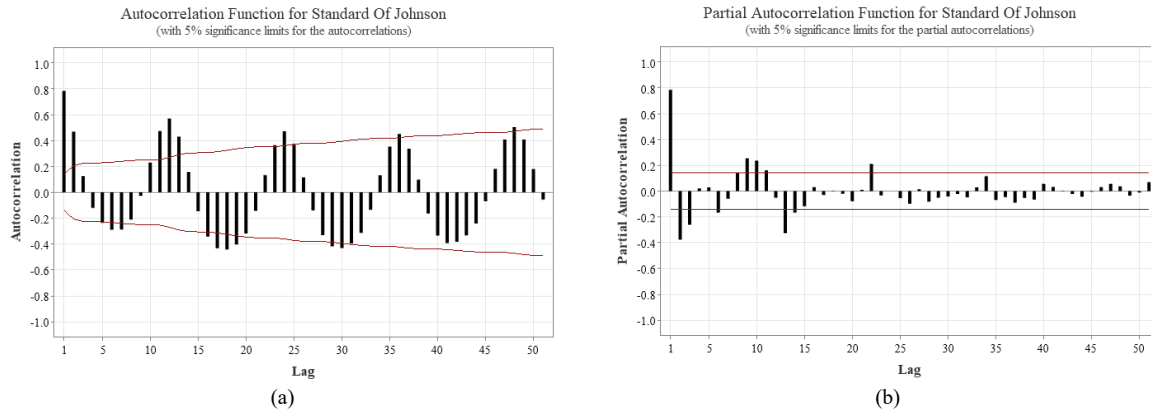


Figure 3. a) ACF and b) PACF for observed data of Chalus River Flow Rate

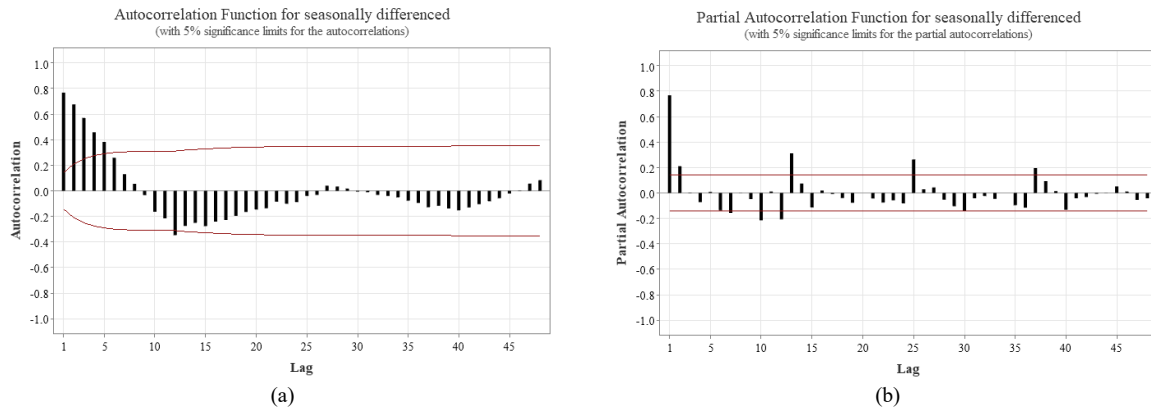


Figure 4. a) ACF, and b) PACF for first order seasonal differencing and de-seasonal observed data of Chalus River Flow Rate

Therefore, SARIMA (p, 0, q) (P, 1, Q)<sub>12</sub> models were considered. The values of the parameters p, q, P, and Q was specified by the characteristics identified in the de-seasonalized ACF and PACF plots (as shown in Figure 4). The ACF plot of the time series in Figure 4-a that has been adjusted for seasonal variations demonstrates a gradual decrease in correlation values, with notable spikes observed at lag positions 1 through 5, while the spikes in ACF plot placed in confidence interval beyond the 5<sup>th</sup> lag, hence the order for the moving average parameter (MA) (non-seasonal component) was put forward as q=0-5. Furthermore, Figure 4-a illustrates a significant downward spike at the 12<sup>th</sup> lag on the ACF plot, surpassing the confidence interval at that lag, and following the 24<sup>th</sup> lag, the ACF spikes decreased and fell within the ACF confidence interval, leading to a suggested order of Q=1 for seasonal moving average (SMA) values.

Similarly, in the non-seasonal factor, the PACF plot of the de-seasonal observed data of Chalus River flow rate as illustrated in Figure 4-b displays notable peaks at the first and second lags, with the confidence interval of the PACF plot being cutts off, and then the spikes are in range of confidence interval after lag 2<sup>nd</sup>, consequently, the recommended value for the autoregressive (AR) parameter

is p=0-2. Moreover, Figure 4-b displays notable peaks at the 12<sup>th</sup>, 24<sup>th</sup> and 36<sup>th</sup> lags on the PACF plot, positioned outside the confidence interval lines, leading to the suggestion of P=0-3 for the seasonal autoregressive (SAR) parameters.

Subsequently, SARIMA models were considered for additional assessment according to the specified criteria outlined in Table 5, which mong them, SARIMA(2,0,0)(0,1,1)<sub>12</sub> determined to be the most optimal model owing to its lowest AIC value.

Upon the selection of the appropriate model, it becomes essential to examine the residuals of the model to ensure its accuracy. Consequently, the modified Ljung-Box test was utilized to assess the model's adequacy and the randomness of the residuals. The modified Ljung-Box test outcomes in Table 6 demonstrate that the residuals are independent, given that the p-value exceeds 0.05 for all delays, furthermore the absence of significant autocorrelation in all residual values is evident from the ACF and PACF plots shown in Figure 5.

The Anderson Darling test, the normal probability diagram, and the histogram of the residuals were employed to assess the normality of the residuals. With a p-value of 0.4 from the Anderson Darling test, it can be inferred that

the residuals exhibit normality; moreover, the visual representations in Figures 6-a and 6-c further confirm this normality. Additionally, Figure 6-b points to a consistent variance in the residuals. The plot in Figure 6-b displays the relationship between residuals and fitted values, supporting the assumption that the residuals exhibit consistent variance. The data points in Figure 6-c are distributed randomly around zero without any clear trends, indicating consistent residual variance. Also, the Run Test's validation indicates the randomness of the residuals, as the p-value is above 0.05.

The SARIMA(2,0,0)(0,1,1)<sub>12</sub> model's accuracy was validated through an examination that included the squared criteria of the correlation coefficient, error percentage, and Nash Sutcliffe efficiency coefficient, detailed in Table 7. The results presented in Table 7 demonstrates that the SARIMA model for Chalus River Flow Rate exhibits satisfactory accuracy.

The graph depicted in Figure 7 illustrates the monthly Chalus River Flow Rate through historical and prediction data based on a SARIMA (2, 0, 0) (0, 1, 1)<sub>12</sub> model. Moreover, the out-of-sample predict graph exhibits a similar trend to the validation and historical graphs, but it falls short in predicting exceptionally high flows. In general the chosen model is suitable for predicting Chalus River flow rate for future conditions. The order of p being 2 in the SARIMA (2, 0, 0) (0, 1, 1)<sub>12</sub> model implies that the Chalus River flow rate time series ( $y_t$ ) is connected to its earlier data points  $y_{t-1}$ , and  $y_{t-2}$ , With an order Q of 1,  $y_t$  is influenced by the preceding random shocks of  $\varepsilon_{t-12}$ . Since the non-seasonal part of the model was already stationary, there was no need to apply non-seasonal differencing ( $d=0$ ), nevertheless, seasonal differencing was employed just once to eliminate seasonal patterns in the model.

**Table 5. Optional SARIMA models for Chalus River Flow Rate**

Model (d = 0, D = 1)	AIC	Model (d = 0, D = 1)	AIC	Model (d = 0, D = 1)	AIC
<b>p = 2, q = 0, P = 0, Q = 1*</b>	<b>220.87</b>	p = 2, q = 4, P = 2, Q = 1	296.89	p = 1, q = 4, P = 1, Q = 1	324.36
p = 2, q = 1, P = 0, Q = 1	222.86	p = 2, q = 3, P = 2, Q = 1	300.99	p = 2, q = 4, P = 1, Q = 1	328.74
p = 2, q = 0, P = 1, Q = 1	225.69	p = 2, q = 4, P = 0, Q = 1	301.24	p = 0, q = 5, P = 2, Q = 1	337.26
p = 1, q = 0, P = 0, Q = 1	232.63	p = 0, q = 4, P = 2, Q = 1	303.04	p = 0, q = 2, P = 2, Q = 1	347.22
p = 1, q = 0, P = 1, Q = 1	236.08	p = 1, q = 3, P = 0, Q = 1	306.08	p = 1, q = 5, P = 0, Q = 1	359.12
p = 2, q = 2, P = 1, Q = 1	235.9	p = 2, q = 0, P = 3, Q = 1	306.91	p = 1, q = 1, P = 2, Q = 1	359.64
p = 2, q = 1, P = 1, Q = 1	236.84	p = 1, q = 2, P = 0, Q = 1	307.56	p = 2, q = 5, P = 0, Q = 1	363.3
p = 1, q = 0, P = 2, Q = 1	261.57	p = 1, q = 1, P = 1, Q = 1	311.49	p = 1, q = 5, P = 1, Q = 1	368.88
p = 2, q = 2, P = 0, Q = 1	271.19	p = 1, q = 4, P = 0, Q = 1	312.32	p = 0, q = 3, P = 2, Q = 1	370.62
p = 1, q = 1, P = 0, Q = 1	282.01	p = 2, q = 4, P = 3, Q = 1	313.3	p = 0, q = 4, P = 3, Q = 1	371.58
p = 2, q = 1, P = 2, Q = 1	281.81	p = 2, q = 3, P = 1, Q = 1	317.45	p = 1, q = 2, P = 2, Q = 1	386.35
p = 2, q = 3, P = 3, Q = 1	290.01	p = 1, q = 2, P = 1, Q = 1	319.69	p = 0, q = 1, P = 3, Q = 1	387.45
p = 2, q = 1, P = 3, Q = 1	291.58	p = 2, q = 3, P = 0, Q = 1	320.43	p = 2, q = 5, P = 1, Q = 1	387.56
p = 1, q = 0, P = 3, Q = 1	293.09	p = 1, q = 3, P = 1, Q = 1	321.3	p = 1, q = 2, P = 3, Q = 1	388.76

**Table 6. The results of Modified Box-Pierce (Ljung-Box) Chi-Square Statistic**

Lag	12	24	36	48
Chi-Square	5.51	16.85	29.35	31.42
DF	9	21	33	45
P-Value	0.788	0.720	0.649	0.938

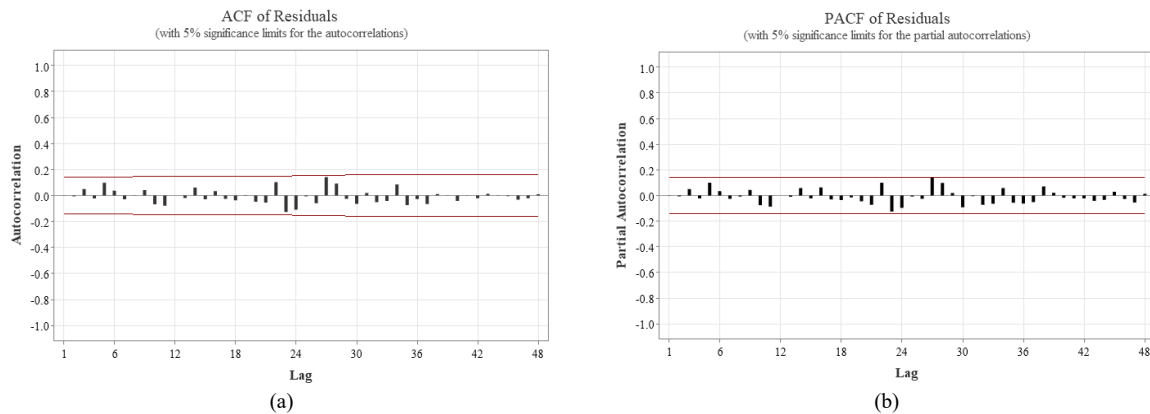


**Figure 5. a) ACF, and b) PACF of residuals for Chalus River Flow Rate model**

### Residual Plots for Standard Of Johnson

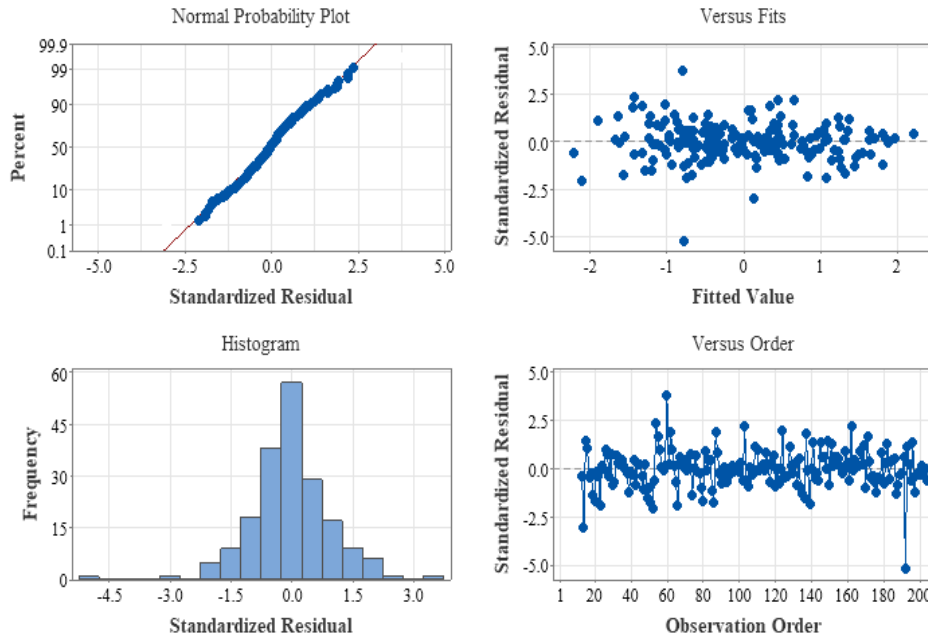


**Figure 6.** a) Normal probability plot, b) Histogram plot, c) Residuals versus fitted value plot, d) RUN-test plot of residuals of Chalus River Flow Rate model

**Table 7.** Precision criteria for Chalus River Flow Rate model

$R^2$	E%	NS
0.91	2.68	0.77

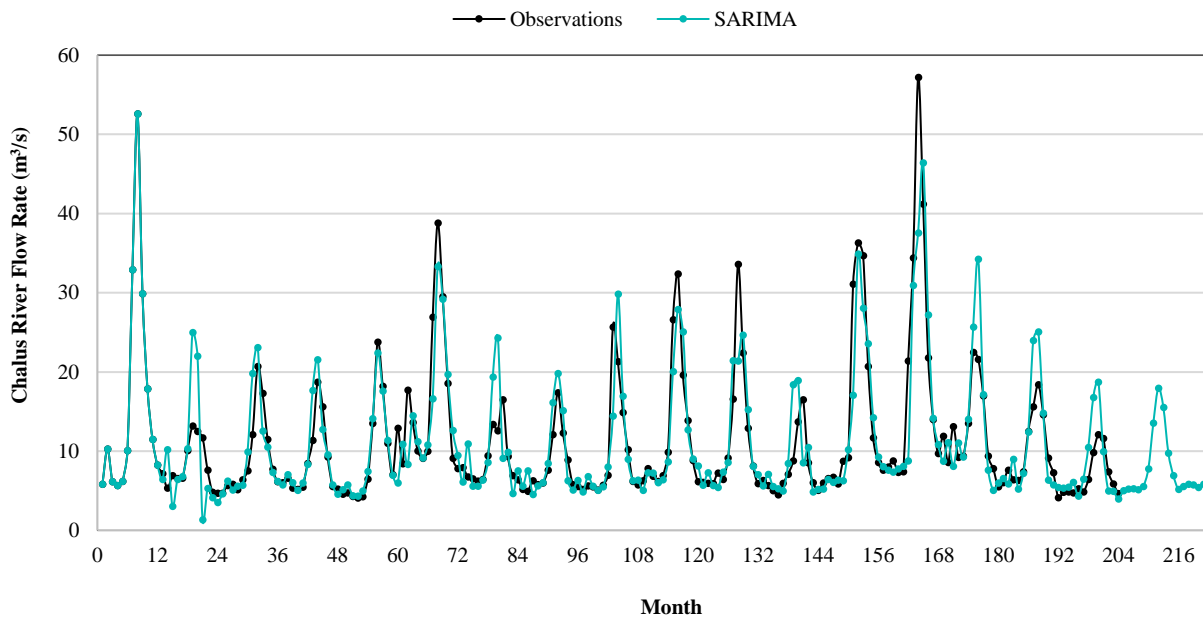


**Figure 7.** Observed and predicted Flow Rate of Chalus River

## 4. Conclusions

The primary aim of this research is to predict the Chalus River's water flow in Mazandaran Province, Iran, by employing SARIMA model with monthly data spanning from 2006 to 2023. Data analysis was carried out at the Pol Zoghal station to make predictions regarding flow rates in the year 2024. The study makes a valuable contribution to

the continuous exploration of SARIMA model applications in hydrological forecasting, particularly in regions with substantial seasonal variations. It showcases how SARIMA effectively captures both seasonal and non-seasonal aspects of time series data. To implement the SARIMA model, it is essential to evaluate data stationarity using the Augmented Dickey-Fuller (ADF) test, transform the data through the Johnson Transformation, and deduce SARIMA parameters

(p, d, q)(P, D, Q)<sub>s</sub> based on Autocorrelation Function (ACF) and Partial Autocorrelation Function (PACF) plots. MiniTab software was utilized in the study for SARIMA modeling, alongside the application of various statistical tests for data analysis and validation. The most suitable model for forecasting the monthly flow rates of the Chalus River was found to be SARIMA (2,0,0)(0,1,1)<sub>12</sub>, showing exceptional precision. The model is well-suited for forecasting future flow rates, even if it may not completely capture extreme values.

## 5. References

- [1] Mamudu, L., Yahaya, A., & Dan, S. (2021). Application of seasonal autoregressive integrated moving average (SARIMA) for flows of river kaduna. *Nigerian Journal of Engineering*, 28(2).
- [2] Tadesse, K. B., & Dinka, M. O. (2017). Application of SARIMA model to forecasting monthly flows in Waterval River, South Africa. *Journal of Water and Land Development*, 35(1), 229–236. doi:10.1515/jwld-2017-0088.
- [3] Rahmani Firozjaei, M., Salehi Neyshabouri, S. A. A., Amini Sola, S., & Mohajeri, S. H. (2018). Numerical Simulation on the Performance Improvement of a Lateral Intake Using Submerged Vanes. *Iranian Journal of Science and Technology, Transactions of Civil Engineering*, 43(2), 167–177. doi:10.1007/s40996-018-0126-z.
- [4] Rahmani Firozjaei, M., Behnamtalab, E., & Salehi Neyshabouri, S. A. A. (2019). Numerical simulation of the lateral pipe intake: flow and sediment field. *Water and Environment Journal*, 34(2), 291–304. doi:10.1111/wej.12462
- [5] Dadkhah Tehrani, M., Karimi Darmian, S., Moridi, A., & Khalili, R. (2023). Evaluation of water quality of Chalus River based on IRWQIsc and NSFQI water quality index. *Journal of Environmental Science Studies*, 8(3), 7064–7072.
- [6] Phan, T.-T.-H., & Nguyen, X. H. (2020). Combining statistical machine learning models with ARIMA for water level forecasting: The case of the Red river. *Advances in Water Resources*, 142, 103656. doi:10.1016/j.advwatres.2020.103656.
- [7] Wang, W. chuan, Chau, K. wing, Xu, D. mei, & Chen, X. Y. (2015). Improving Forecasting Accuracy of Annual Runoff Time Series Using ARIMA Based on EEMD Decomposition. *Water Resources Management*, 29(8), 2655–2675. doi:10.1007/s11269-015-0962-6.
- [8] Azad, A. S., Sokkalingam, R., Daud, H., Adhikary, S. K., Khurshid, H., Mazlan, S. N. A., & Rabbani, M. B. A. (2022). Water Level Prediction through Hybrid SARIMA and ANN Models Based on Time Series Analysis: Red Hills Reservoir Case Study. *Sustainability*, 14(3), 1843. <https://doi.org/10.3390/su14031843>.
- [9] Mombeni, H. A., Rezaei, S., Nadarajah, S., & Emami, M. (2013). Estimation of Water Demand in Iran Based on SARIMA Models. *Environmental Modeling & Assessment*, 18(5), 559–565. doi:10.1007/s10666-013-9364-4.
- [10] Sheikholeslami, Z., Ehteshami, M., & Nazif, S. (2024). Development of a System Dynamics Model for Prediction of Karaj Reservoir Share in Tehran Water Supply. *Numerical Methods in Civil Engineering*, 8(2), 22–35. doi:10.61186/nmce.2303.1029.
- [11] Gharde, K. D., Kothari, M., & Mahale, D. M. (2016). Developed Seasonal ARIMA Model to Forecast Streamflow for Savitri Basin in Konkan Region of Maharashtra on Daily Basis. *J. Indian Soc. Coastal Agric. Res*, 34(1), 110–119.
- [12] Katimon, A., Shahid, S., & Mohsenipour, M. (2018). Modeling water quality and hydrological variables using ARIMA: a case study of Johor River, Malaysia. *Sustainable Water Resources Management*, 4(4), 991–998. doi:10.1007/s40899-017-0202-8.
- [13] Kassem, A. A., Raheem, A. M., & Khidir, K. M. (2020). Daily Streamflow Prediction for Khazir River Basin Using ARIMA and ANN Models. *Zanco Journal of Pure and Applied Sciences*, 32(3). doi:10.21271/zjpas.32.3.4.
- [14] Adams, S. O., Bamanga, M., & Ardo Bamanga, M. (2020). Modelling and Forecasting Seasonal Behavior of Rainfall in Abuja, Nigeria; A SARIMA Approach. *American Journal of Mathematics and Statistics*, 2020(1), 10–19. doi:10.5923/j.ajms.20201001.02.
- [15] Tao, H., Sun, Q., Wu, R., Zeng, X., & Liu, X. (2024). Predictive Analysis of Yellow River Water and Sand Monitoring Data Based on the ARIMA Model. *Proceedings - 2024 International Conference on Electrical Drives, Power Electronics and Engineering, EDPEE 2024*, 82, 575–579. doi:10.1109/EDPEE61724.2024.00113.
- [16] Ning, Y. Z., & Musa, S. (2023). Stream Flow Forecasting on Pahang River by Time Series Models, ARMA, ARIMA and SARIMA. *Recent Trends in Civil Engineering and Built Environment*, 4(1), 331–341. <http://publisher.uthm.edu.my/periodicals/index.php/rtcebe>
- [17] Mazandaran Regional Water Company. (2024). Report on the status of water resources in Mazandaran province, Mazandaran Regional Water Company, Sari, Iran.
- [18] K, Dimri, T., Ahmad, S., & Sharif, M. (2020). Time series analysis of climate variables using seasonal ARIMA approach. *Journal of Earth System Science*, 129(1). doi:10.1007/s12040-020-01408-x.
- [19] Sirisha, U. M., Belavagi, M. C., & Attigeri, G. (2022). Profit Prediction Using ARIMA, SARIMA and LSTM Models in Time Series Forecasting: A Comparison. *IEEE Access*, 10, 124715–124727. doi:10.1109/ACCESS.2022.3224938.
- [20] Obateru, R. O., Adeyefa, A. O., & Fashae, O. A. (2023). Drought assessment and rainfall trend analysis in southwestern Nigeria. *World Water Policy*, 9(2), 254–273. doi:10.1002/wwp2.12102.
- [21] Jin, J., Wang, G., Zhang, J., Yang, Q., Liu, C., Liu, Y., Bao, Z., & He, R. (2020). Impacts of climate change on hydrology in the Yellow River Source Region, China. *Journal of Water and Climate Change*, 11(3), 916–930. doi:10.2166/wcc.2018.085.

- [22] Muia, V. K., Opere, A. O., Ndunda, E., & Amwata, D. A. (2024). Rainfall and Temperature Trend Analysis using Mann-Kendall and Sen's Slope Estimator Test in Makueni County, Kenya. *J. Mater. Environ. Sci.*, 15 (3), 349, 367.
- [23] Kabbilawsh, P., Kumar, D. S., & Chithra, N. R. (2023). Assessment of temporal homogeneity of long-term rainfall time-series datasets by applying classical homogeneity tests. *Environment, Development and Sustainability*, 26(7), 16757–16801. doi:10.1007/s10668-023-03310-0.